Estuarine, Coastal and Shelf Science 243 (2020) 106904

Contents lists available at ScienceDirect

Estuarine, Coastal and Shelf Science

journal homepage: www.elsevier.com/locate/ecss

On the effect of climate trends in coastal density on deep water renewal frequency in sill fjords—A statistical approach

E. Darelius

Geophysical Institute, University of Bergen and the Bjerknes Centre for Climate Research, Bergen, Norway

ARTICLE INFO

Keywords:
Sill fjord
Deep water renewal
Stagnation period
Ocean warming

ABSTRACT

The basin water of a sill fjord is renewed intermittently, when the density of the water at sill level in the ocean outside the fjord is high enough for it to sink down to the bottom of the fjord. How often the basin water is renewed, the renewal frequency, depends on how fast diffusion and mixing cause the density in the basin to decrease and on the variability of the density in the ambient ocean. Here, we suggest a statistical approach to investigate how a trend – e.g. imposed by global warming – in the ambient ocean density will affect the renewal frequency of a sill fjord. Negative ambient trends that are large compared to the rate at which density decreases the fjord will have large impact on the renewal frequency. It is shown that the observed negative trend in the annual maximum density at a hydrographical station near the Norwegian fjord Masfjorden, is very likely to have reduced the renewal frequency and increased the length of the stagnation period compared to pre-trend conditions. Negative trends in the annual maximum density since 1990 are observed at six out of eight longterm hydrographical stations along the Atlantic Norwegian coast, suggesting that the deep water renewal frequency in many Norwegian fjords has been reduced during the last 30 years.

1. Introduction

Fjords are long and narrow, steep-sided and glacially carved inlets that are found at high latitudes in both hemispheres. A fjord typically has one or many sills, which isolates the deep waters of the fjord basin(s) from the coastal waters outside the sill (Fig. 1c). The basin water, i.e. the water below sill level is only exchanged (or renewed) when the density of the coastal water at sill level outside the fjord (ρ_{coast}) exceeds that of the stagnant water within the basin (Gade and Edwards, 1980). Diffusion and mixing will reduce the density of the basin water with time (e.g. Stigebrandt and Aure, 1989), allowing for a renewal of the basin water to take place. The mean length of the stagnation period, i.e. the interval between two renewals, varies greatly between fjord systems and ranges from a few weeks (e.g. Gillibrand et al., 1995) to many years (Gade and Edwards, 1980). In a poorly ventilated fjord, biological activity will with time consume the available oxygen, leaving the basin waters in an hypoxic or even anoxic state (e.g. Gillibrand et al., 1996). If the length of stagnation periods for some reason were to increase, we can therefore expect the water quality in the deeper part of the fjord to be reduced. In the Gullmar fjord, Sweden, for example, the renewal rate is tightly linked to the NAO-index, with long periods of positive NAO leading to fewer renewals, hypoxic conditions and changes in the fjord eco-system (Polovodova Asteman and Nordberg, 2013).

Further to the north, in the Norwegian fjord Masfjorden (Fig. 1a–b) oxygen concentrations has been observed to decrease in recent years, causing authorities to question its suitability for e.g. fish farming. Aksnes et al. (2019) suggest that the changes are caused by a reduction in the density of the coastal waters, which has led to reduced ventilation rates (i.e. longer periods of stagnation) and decreased oxygen concentrations in the basin waters of the fjord. They apply a simplistic empirical model to infer the evolution of the oxygen concentration in the fjord, in which the annual renewal rate of the fjord, i.e. the percentage of the basin water that is renewed with high oxygen open ocean water in a year, increases linearly as a function of what they call the "high density frequency", or the percentage of times that the density at sill depth at a nearby hydrographic station (observed quasi bi-weekly) is above a certain threshold. Aksnes et al. (2019) used a constant threshold ($\rho_0 = 1027.75$ kg m^3) based on the observed average density of Masfjorden in the period 1975–2017. The "high density frequency" has decreased since the 70s, leading to reduced ventilation rates and lower oxygen concentration in Aksnes et al.'s (2019) model. The predictions from the simple model match observed oxygen levels in the fjord basin relatively well.

When the open ocean conditions are changing, e.g. in the presence of a long-term trend, it evidently becomes problematic to use a fixed density criteria to determine the renewal rate, as the density in the fjord basin depends on and will evolve with the open ocean density.

E-mail address: elin.darelius@uib.no.

https://doi.org/10.1016/j.ecss.2020.106904
Received 15 January 2020; Received in revised form 15 May 2020; Accepted 19 June 2020
Available online 22 June 2020

Consider, for simplicity, a case where the coastal density drops so that the density no longer reaches above the threshold. The fjord density will decrease (due to diffusion) and at some point the density of the coastal water will be high enough for renewal to take place, even if $\rho_{coast} < \rho_0$.

We will here re-visit Masfjorden and the data sets used by Aksnes et al. (2019), but following Gade (1973) we will take a statistical approach to evaluate to what degree the observed trend in the density of the coastal waters would affect the renewal rate of the deep water in fjords such as e.g. Masfjorden. The proposed statistical framework can be applied to other fjord areas where coastal densities show a trend, for example Northeast Greenland, where the coastal waters have been freshening since 2003 (Sejr et al., 2017), potentially halting deep water renewal rate in the Young Sound-Tyrolerfjord in Northeast Greenland (Boone et al., 2018). The framework can also be used to infer future changes in fjord water quality based scenarios from numerical models that do not resolve the small-scale fjord topography.

The framework does not allow for partial renewals (see Section 4) and it cannot be applied to e.g. fjords on Svalbard where deep water renewal is caused by convection during winter (Cottier et al., 2010), or to fjords where deep water renewal is a continuous process, such as e.g. in the Ilulissat Icefjord in western Greenland (Gladish et al., 2015).

2. Theory

We review and build on the work by Gade (1973) and consider the deep water renewal in a fjord to be a stochastic process depending on the statistical properties of the density variations outside of the sill. In order to do so, we assume that:

1. the stagnant deep water in the fjord is homogeneous and that its density (ρ_{fjord}) decreases linearly with time at a rate $-D$ kg m^{-3} yr^{-1} due to diffusion and vertical mixing.
2. Deep water is renewed when the density outside the sill at sill depth (ρ_{coast}) is higher than ρ_{fjord}. The renewal is total and instantaneous, so that when the water is renewed we get $\rho_{coast} = \rho_{fjord}$.
3. In a particular year, the deep water is either renewed or it is not, and so the stagnation period N is an integer number of years.

If ρ_{coast} can be described as a stochastic variable with a probability density function $g(\rho_{coast})$, then the density of the basin water just after renewal ρ will also be a stochastic variable with its own probability density function $f(\rho)$, which is such that

$$\int_0^{\infty} f(\rho_0)\, q(\rho|\rho_0)\, d\rho_0 \;=\; f(\rho), \qquad 0 < \rho < \infty, \tag{1}$$

where ρ_0 is any initial condition and $q(\rho|\rho_0)$ is the probability density function for the density of the next renewal given ρ_0 (Gade, 1973).

While Gade (1973) solved Eq. (1) numerically, we take a Monte Carlo approach and simulate a large number ($n = 10^6$) of deep water renewals in order to obtain $f(\rho)$ for a given $g(\rho_{coast})$, which we for simplicity take to be normally distributed with a mean μ and a standard deviation σ.

For an initial fjord density ρ_* (renewed at $n = 0$ year), we "draw" a random sample $\rho_{coast,1}$ from the coastal distribution $g(\rho_{coast})$ and compare it with the fjord density at $n = 1$ year, which is $\rho_{basin,1} = \rho_* - Dn$. If $\rho_{coast,1}$ is smaller than $\rho_{basin,1}$, then there is no renewal and we repeatedly draw new samples ("once a year") until after n^* years we have

$$\rho_{coast,n^*} > \rho_{basin,n^*} = \rho_* - n^* D \tag{2}$$

and the fjord water is renewed. The process is started over, with the new $\rho_* = \rho_{coast,n^*}$.

Fig. 2a shows the normalized probability distributions $f(\rho)$ obtained for various values of D/σ, and we note, just like Gade (1973), that the density within the fjord is higher and less variable than the density along the coast outside. This tendency increases for decreasing values of D/σ and at the same time, the mean length of the stagnation period (the interval between two renewals) increases (Figs. 2b and 3a). Gade (1973) found that the mean stagnation period, $\overline{N}$, can be described by

$$\overline{N} = 1 + 0.729\left(\frac{D}{\sigma}\right)^{-\sqrt{3}/2} \tag{3}$$

for D/σ in the range $\sqrt{2}/80 < D/\sigma < \sqrt{2}/2.5$.

Our results fall on this line for low values of D/σ, but are about 10% lower for the higher values of D/σ, potentially due to numerical errors in Gade's (1973) calculations.

Now, how does these results change if we after $n = n_0$ years superimpose a trend (α kg m^{-3} yr^{-1}) in the density of the coastal waters, such that for $n > n_0$ we have $\mu(n) = \mu(0) + \alpha(n - n_0)$?

We repeat the process described above, but (i) the initial density ρ_* is now drawn from the corresponding distribution obtained without a trend ($f(\rho)$) and (ii) the fjord density $\rho_* - nt_0 D$ is compared with the coastal density $\rho_{coast,n} + \alpha n$, i.e. we have $n_0 = 0$ years (where $\rho_{coast,n}$ is drawn from $g(\rho_{coast})$ as in the example without a trend). The fjord water is renewed if

$$\rho_{coast,n} + \alpha n > \rho_* - nD, \tag{4}$$

or, rewritten in the form of Eq. (2)

$$\rho_{coast,n} > \rho_* - nD^*, \tag{5}$$

where $D^* = D + \alpha$. The results obtained above can hence be applied to a situation with a trend in the coastal density if we replace D by D^*.

Fig. 3 shows how a trend $\alpha = kD$ impacts the length of the stagnation periods. As expected, positive trends (positive k) will decrease the length of the stagnation period and negative trends (negative k) will increase it. The effect of negative trends are larger than the effect of a positive trend. A small trend (small relative to D, i.e. $|\alpha| \ll D$ or $|k| \ll 1$), will have little effect on the expected stagnation period. If $\alpha < -D$ i.e. for $k < -1$ or $D^* < 0$, then renewal will stop altogether, since the density outside of the fjord then decreases faster than the density within the fjord (not shown).

3. Masfjorden: An example from the Norwegian west coast

Masfjorden (60°51′53″ N 05°21′23″E, Fig. 1) is a 24 km long and 0.5–2 km wide side-fjord to Fensfjorden, located on the west coast of Norway. The main sill depth is 75 m and the deepest basin is about 470 m deep. Masfjorden is regularly discussed in regional media as recent observations of low-oxygen conditions in the deep, stagnant basin waters (Aksnes et al., 2019) are suggested to be caused by fish-farming activities inside the fjord.

There exist quasi-annual hydrographic profiles from the inner, deep basin since 1990 (data available from International Council for the Exploration of the Sea and Norwegian Marine Data Center) and the temporal evolution of bottom density (Fig. 4) suggests intermittent deep water renewals separated by multi-year-long stagnant periods during which the bottom density decreases with time. Since the observations started in 1990 there have been at least five deep water renewals (red circles in Fig. 4) and the length of the stagnation periods has been in the range 2–10 years. The density decrease during the stagnant periods suggests D = 0.010–0.015 kg m^{-3} yr^{-1}. These values are slightly lower than the values given by Aksnes et al. (2019), who considered the basin average density while we use the bottom density.

The basin volume (below sill depth) in Masfjorden is about 0.4 km^3 and the strait above the sill can be approximated by a 600 m wide and 70 m deep rectangle. Following Arneborg et al. (2004) it would take 1–3 days to renew the deep water if the density difference is 0.06 kg m^3 (as it was for the renewal in 2005, Fig. 4), the surface layer is 10 m and the flow is frictionally balanced. Following the classification of Stigebrandt (2012), Masfjorden is hence a "mixing system", where

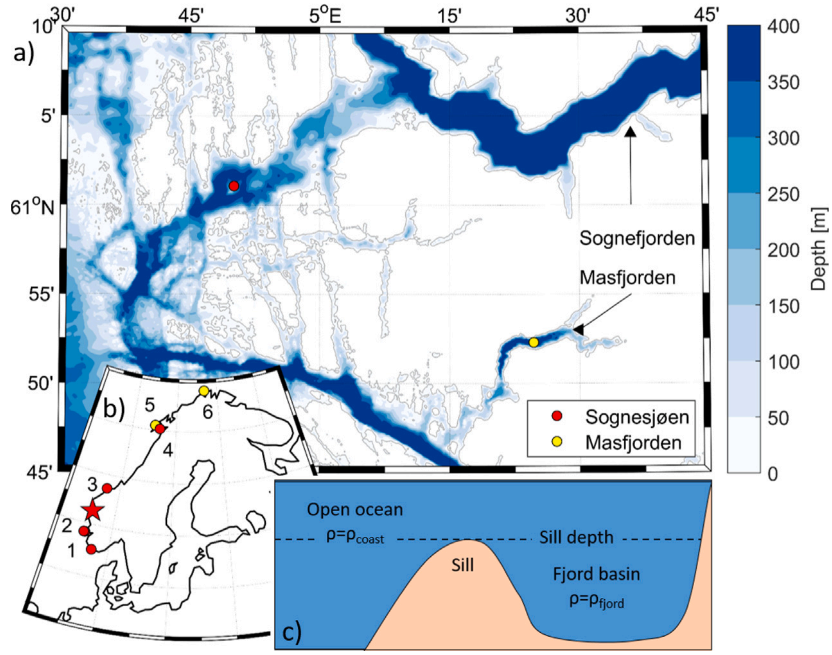

Fig. 1. (a) Map showing the bathymetry (blue shading) and location of Masfjorden and the hydrographic station Sognesjøen. The positions of the repeated CTD-stations are marked with colored dots according to the legend. The color scale is cut at 400 m—The Sognefjord is over 1000 m deep. The inset (b) shows the location of the study area (red star) and the other hydrographic stations along the Norwegian coast: (from south) Lista (1), Inner and outer Utsira (2), Bud (3), Skrova (4), Eggum (5) and Ingøy (6). Stations showing a significant trend in density after 1990 (Table 2) are shown in red (Stations 1–4 and Sognesjøen) and stations with no significant trend are shown in yellow (stations 5–6) c) Sketch of a fjord basin. (For interpretation of the references to color in this figure legend, the reader is referred to the web version of this article.)

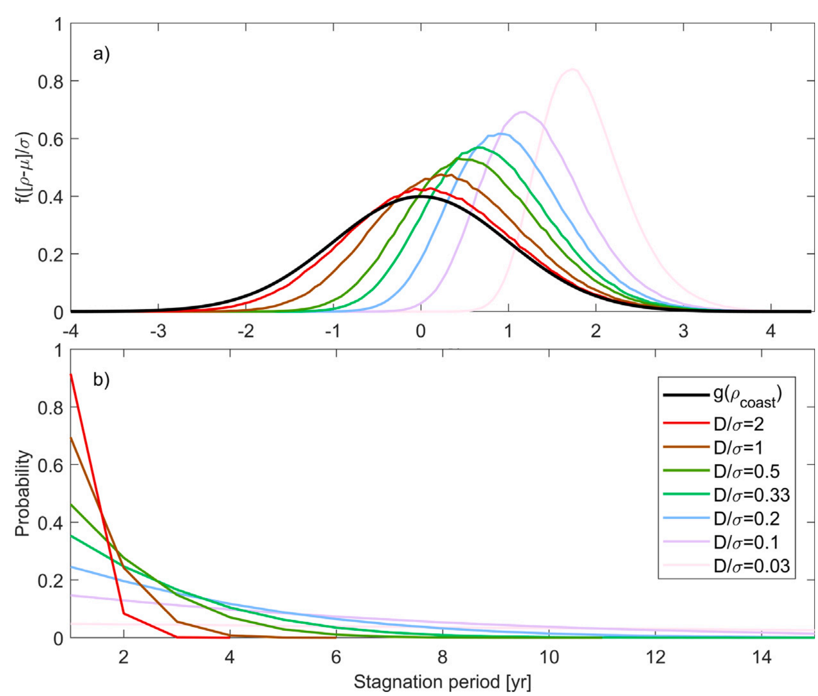

Fig. 2. (a) Non-dimensional probability distributions of inflow density $f(\rho)$ for different values of D/σ according to the legend. The probability distribution outside of the sill $g(\rho_{coast})$ is shown for reference (black line) and (b) probability distribution for the length of the stagnation periods.

the length of the stagnant periods are determined by the rate of mixing and the density variability outside the fjord sill. This suggests that the method described in Section 2 would be applicable to Masfjorden. To do so, we need information about the density variability outside the fjord $g(\rho_{coast})$.

3.1. Variability and trends on the continental shelf

There are limited data available from the area directly outside of the sill of Masfjorden, and instead we turn (following Aksnes, 2019) to the hydrographical station "Sognesjøen" (61°01′04″N 04°50′04″E),

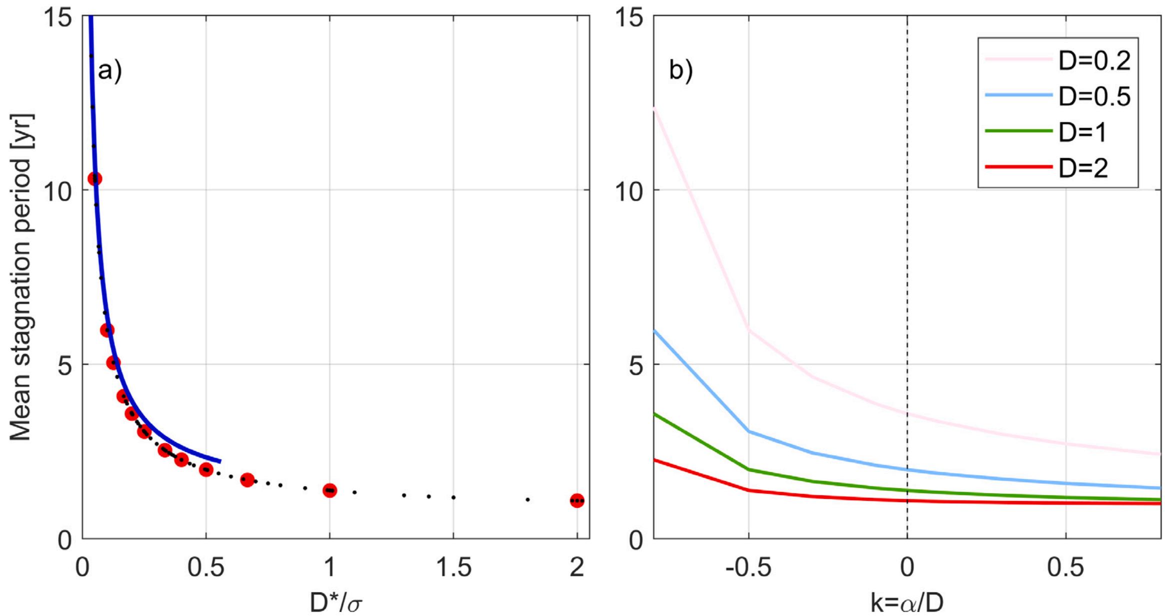

Fig. 3. (a) Mean length of the stagnation period $\overline{N}$ as a function of $D^*/\sigma = (D+\alpha)/\sigma$: results from runs without trend (large, red dots), with trend (small, black dots) and the relation given in Gade (1973), Eq. (3) (blue line). (b) $\overline{N}$ for different values of $k = \alpha/D$ and D/σ (according to the legend). k=0 is highlighted with a dashed line. (For interpretation of the references to color in this figure legend, the reader is referred to the web version of this article.)

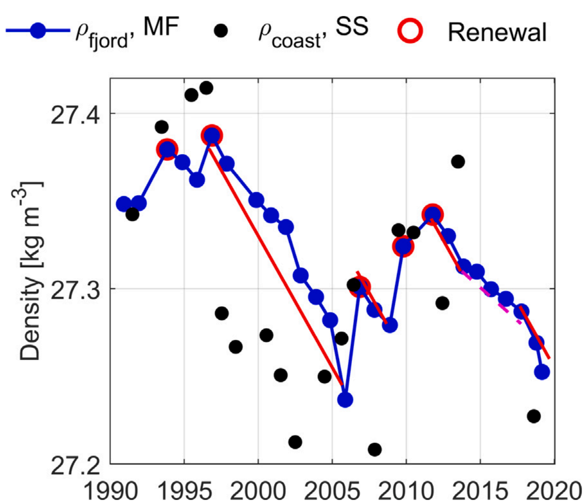

Fig. 4. Time series of density (ρ - 1000) at the bottom (470 m depth) of the inner, deep basin of Masfjorden. The straight, colored lines are reference lines to show the density decrease using the suggested values for D, D = −0.015 kg m^{-3} yr^{-1} (red) and D = −0.010 kg m^{-3} yr^{-1} (magenta, dashed line). Black circles show observed maximum density in Sognesjøen in between the occupations in Masfjorden; years without black circles have maximum densities outside (below) the shown density range. (For interpretation of the references to color in this figure legend, the reader is referred to the web version of this article.)

situated about 30 km northwest of Masfjorden (Fig. 1a) where quasi-bi-weekly observations of temperature and salinity are available since 1935 (data available at Norwegian Institute of Marine Research). The depth at "Sognesjøen" is 400 m, but there is a sill of about 200 m further out that restricts circulation at greater depths. Above sill depth, however, water can circulate freely between Sognesjøen and the sill of Masfjorden, and we assume that the conditions here are representative for the area outside of the Masfjorden sill.

The density at Sognesjøen at 75 m depth (i.e. the sill depth of Masfjorden) is highly variable (Fig. 5) and shows influences from

Table 1
Statistical properties derived from the observed maximum annual density ($\rho - 1000$) at Sognesjøen in the period 1935–1990 (no trend) and 1990–2019 (trend).

Depth [m]	1935–1990		1990–2019		
	μ [kg m^{-3}]	σ [kg m^{-3}]	a_{+rho} [kg m^{-3} yr^{-1}]	p	$\sigma_{detrended}$[a]
75	27.33	0.059	−0.006	0.001	[0.059 0.099]
100	27.39	0.048	−0.005	0.001	[0.054 0.091]
125	27.45	0.045	−0.005	0.003	[0.052 0.087]
150	27.47	0.047	−0.004	0.02	[0.051 0.086]
200	27.49	0.047	−0.003	0.01	[0.051 0.086]
250	27.50	0.048	−0.003	0.05	[0.055 0.093]
300	27.52	0.048	−0.003	0.02	[0.048 0.081]

[a] 95% confidence interval.

both Norwegian coastal water (salinity<34.5) and North Atlantic water (salinity>35). For each year we identify the maximum observed density (Fig. 5b), typically occurring during the summer months (May–August). Prior to about 1990 this quantity varies around a mean of μ = 1027.33 kg m^{-3} (σ = 0.059 kg m^{-3}, Table 1, Fig. 6), while later years shows a negative trend of a_ρ = −0.006 kg m^{-3} yr^{-1} (unless stated otherwise, given trends are significant at 95% significance level), i.e. a decrease of about 0.2 kg m^{-3} over the thirty year period. The decrease in density is observed at all investigated depths (Table 1) although trends weaken with increasing depth. The decrease in density appears to be accompanied by increased variability (σ) in the annual density maximum (from 0.059 to 0.099, Table 1), but the increase is not significant at the 95%-level.

3.2. Deep water renewal in Masfjorden

We simulated deep water renewal in Masfjorden using the procedure outlined in Section 2 and the observed values for μ (1027.33 kg m^{-3}) and σ (0.059 kg m^{-3}) from Sognesjøen prior to 1990 (Table 1) and the mean value of D (0.0125 kg m−3 yr^{-1}) from Masfjorden. Results for D = 0.015 kg m^{-3} yr^{-1} and D=0.010 kg m^{-3} yr^{-1} are also presented. The obtained probability distribution for the renewal density ($f(\rho)$) is shown in Fig. 7.

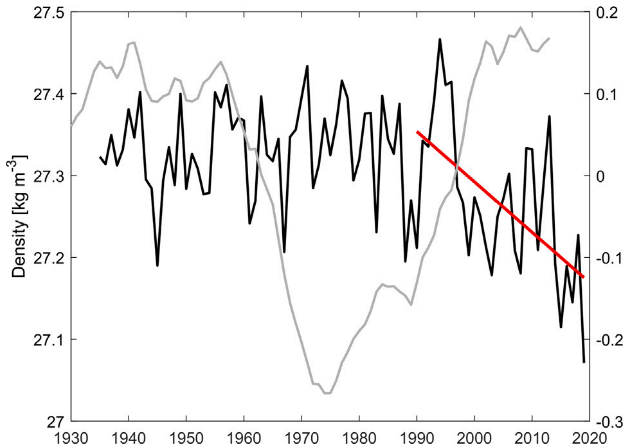

Fig. 5. Time series of observed annual maximum density ($\rho-1000$) at Sognesjøen, 75 m depth (black line, left axis) and the Atlantic Multidecadal Oscillation index (AMO, gray line, right axis). The red line shows the observed trend in density 1990–2019 (α_ρ =-0.006 kg m^{-3} yr^{-1}, significant at 95% significance level). The AMO time series (Enfield et al., 2001) were downloaded from NOAA Earth System Research Laboratory. (For interpretation of the references to color in this figure legend, the reader is referred to the web version of this article.)

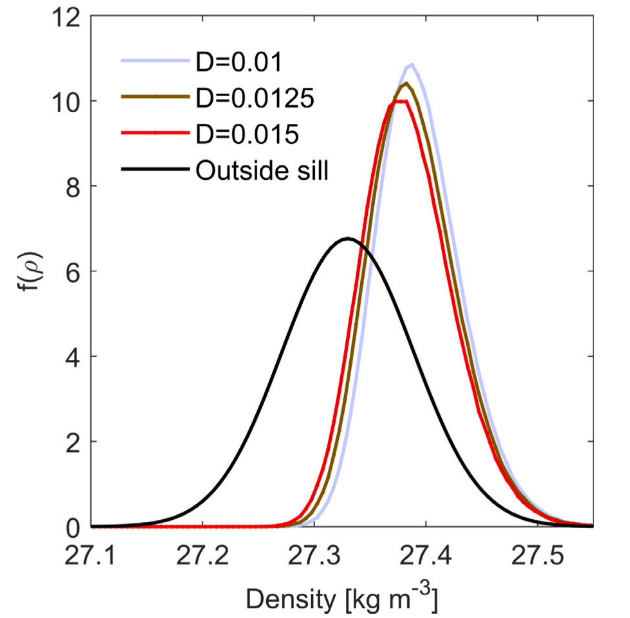

Fig. 7. Probability distributions of the Masfjorden renewal density (ρ – 1000) for observed values of D (Masfjorden), μ and σ from (Sognesjøen, prior to 1990). The probability distribution for annual maximum density from Sognesjøen (from Fig. 6) is shown in black for comparison. (For interpretation of the references to color in this figure legend, the reader is referred to the web version of this article.)

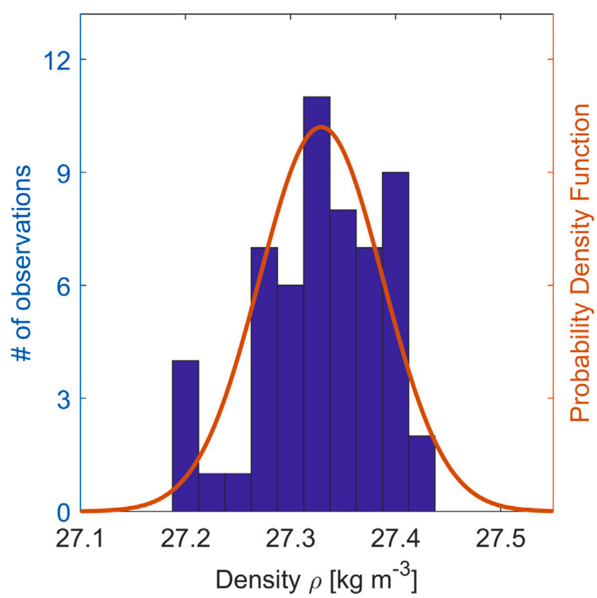

Fig. 6. Histogram showing the distribution of observed annual maximum density (ρ-1000) at Sognesjøen, 75 m depth (n = 56) prior to 1990, and the fitted normal distribution (thick red line) with μ = 27.33 kg m^{-3} and σ = 0.059 kg m^{-3}.

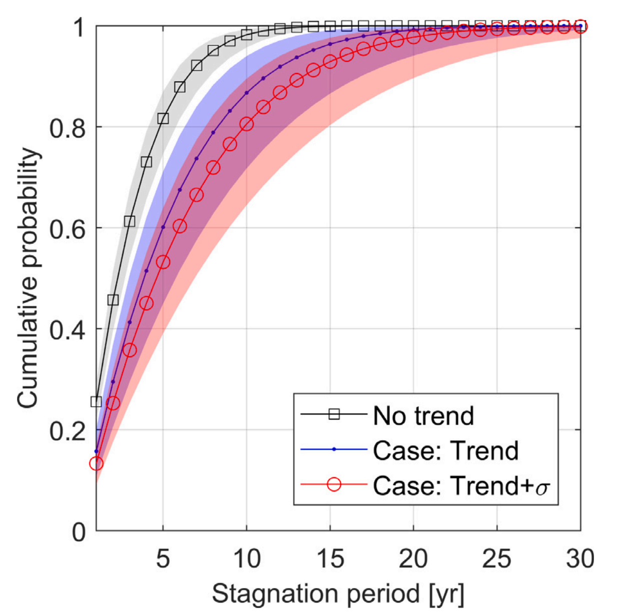

Fig. 8. Cumulative probability distribution for the length of stagnation periods in Masfjorden prior to 1990 (no trend: blue) and after 1990 (case Trend: green, case Trend + σ: red). The shaded area shows results with D in the observed range 0.010–0.015 kg m^3 yr^{-1}. (For interpretation of the references to color in this figure legend, the reader is referred to the web version of this article.)

The exercise was then repeated including (case: Trend) the trend observed after 1990 ($a = -0.006$ kg m^{-3} yr^{-1}) and (case: Trend+σ) the observed trend and the increased variability ($\sigma^* = 0.073$ kg m^{-3}).

When the trend is included, $\overline{N}$ increases from 3.4 (3.0–4.0) years to 5.6 (4.4–8.1) years for case Trend or 6.5 (5.1–9.6) years for case Trend + σ, where the numbers in parentheses gives the results for D = 0.015 and D = 0.010 kg m^{-3} yr^{-1}. Consequently, the "age", i.e. the time that the water beneath sill depth has been in the fjord increases on average and the probability of finding old water in the fjord is higher. For example, the probability of a stagnation period longer than 10 years increases from 0.02 (0.01–0.04) prior to 1990 to 0.13 (0.06–0.28) for case Trend, i.e. roughly with a factor of 6, or to 0.19 (0.10–0.36) for case Trend + σ, i.e. roughly with a factor of 9 (Fig. 8).

Prior to 1990, we would expect on average 8.7 (7.4–9.9) renewals in a 30-year period. For case Trend, 95% (81–99) of the simulated 30 year periods have less than 8.7 renewals and for case Trend + σ more than 99% (92–99) of the simulations have less than 8.7 renewals. It is thus very likely that deep water renewal in Masfjorden has occurred less frequently (compared to the average without trend) during the last 30 years as a result of the warming and freshening trend along the Norwegian coast.

Table 2
Observed trends (after 1990) in annual maximum density at hydrographical stations along the coast of Norway. For location, see Fig. 1b. Only stations and depths at which the trend is significant at 90% is included in the table and trends significant at 95% are marked in bold. No significant trends are observed at Eggum and Ingøy.
Source: Data are available from the Norwegian Norwegian Institute of Marine Research.

Location	Depth [m]	α [kg m^{-3} yr^{-1}]	p-value
1. Lista	50	**−0.005**	0.032
	75	**−0.004**	0.032
	100	**−0.004**	0.009
	150	**−0.003**	0.028
	300[b]	**−0.002**	0.045
2. Indre Utsira	50	**−0.010**	0.006
	75	**−0.008**	<0.001
	100	**−0.005**	0.018
	125[b]	**−0.008**	0.002
2. Ytre Utsira	50	**−0.009**	0.002
	75	**−0.004**	0.02
	100	**−0.006**	0.001
	125	**−0.005**	0.016
	150	**−0.009**	0.01
	200	**−0.008**	0.016
	250[b]	−0.003	0.06
3. Bud	50	−0.007	0.075
	125	−0.004	0.082
	150	**−0.005**	0.047
	200	−0.005	0.067
4. Skrova	150	**−0.004**	0.029
	200	**−0.003**	0.031
	250	**−0.003**	0.03
	300[b]	−0.002	0.068

[b]Bottom.

3.3. Density trends along the Norwegian coast

In addition to Sognesjøen, there are seven more hydrographical stations along the Norwegian coast (Fig. 1) for which temperature and salinity data are available (with shorter and longer gaps) for fixed depths (50, 75, 100, 125, 150, 200, 250, and 300 m are used here) on a quasi-bi weekly basis since the 1940s (Data available from Norwegian Institute of Marine Research). In the following analysis, we have removed data points that where obviously erroneous (salinities>35.4, although flagged good), notably at Lista and Skorva (Stations 1 and 4 in Fig. 1).

While no significant trend in the annual maximum density is observed at the two northernmost stations (Eggum west of Lofoten and Ingøy in the Barents Sea, Stations 5–6 in Fig. 1b), the other five stations show significant trends with the same order of magnitude (and sign) as we observed at Sognesjøen (Table 2).

4. Discussion

Following Gade (1973) we have considered deep water renewal in a sill fjord to be a stochastic process depending solely on the density variability at sill level outside of the sill (σ) and the rate at which vertical mixing cause the density at the bottom of the fjord to decrease ($-D$ kg m^{-3} yr^{-1}). Where the density variability is high and/or the rate at which the fjord density decreases is low, the stagnation periods are long. Motivated by the situation along the west coast of Norway, where we observe a decreasing trend in the annual maximum density of the coastal waters since the early 1990s, we have expanded Gade's (1973) framework to include a trend (α kg m^{-3} yr^{-1}) in the coastal density. We use this expanded theoretical framework to investigate how a trend influences the renewal rate and hence the age of the water in a fjord basin. As expected, imposed trends that are small compared to the density decrease within the fjord ($|\alpha| \ll D$) have little effect, positive trends ($\alpha > 0$) reduce the length of the stagnation periods and negative trends ($\alpha < 0$) increase the length of the stagnation periods. The effect of negative trends on the length of the stagnation period is larger than the effect of positive trends and the extreme case of $\alpha < -D$ will cause deep water renewal to cease altogether. This is likely the current situation in the Young Sound-Tyrolerfjord (74°N) in Northeast Greenland, where the coastal salinities (and thus densities) have been decreasing since 2003 (Sejr et al., 2017). Boone et al. (2018) reports that the salinity at sill level has decreased by 0.11 yr^{-1} between 2003 and 2015, while there was little change in temperature (< 0.01°C) over the same period. The last deep water renewal occurred in 2005, and since then the bottom water salinity in the fjord has decreased by 0.056 yr^{-1} while its temperature increased by 0.17° C over ten years. This gives, if we assume that the annual maximum density has decreased at the same rate as the mean density, $\alpha = -0.09$ kg m^{-3} yr^{-1}, $D =$ 0.05 kg m^{-3} yr^{-1} and $D^* = -0.04$ kg m^{-3} yr^{-1}. Hence, the density of the coastal water decreases more rapidly than that of the basin water and the probability that deep water renewal occurs decreases with time. With more information, e.g. about the coastal density variability (σ) we could have used our statistical framework to say something about the probability for a future deep water renewal (despite the trend), or estimate historical renewal rates in the fjord.

The effect of climate trends in factors other than the coastal hydrography—e.g. in local wind, temperature and precipitation are not explored here, although they can be expected to influence fjord circulation and stratification (Rysgaard et al., 2003), and hence the value of D. If the value of D is increased due to changing climate conditions, it can offset a decreasing trend in the coastal density. On the other hand, if D is decreased, the length of the stagnation periods would increase even further.

As pointed out by Gade (1973), the proposed statistical framework suffers from the limitations imposed by the underlying assumptions (Section 2). Notably, it does not account for partial renewals, i.e. that it is possible that only some fraction of the fjord water is renewed in a given year. It is assumed that a deep water renewal occurs instantaneously and that *all* water below sill depth is replaced. In a real fjord, the basin water will to some extent be stratified, so that the inflowing water might be dense enough to renew only the upper part of the basin water. The results by Aksnes et al. (2019) suggests that this happens regularly in Masfjorden. In addition, the period that the density at sill level is high enough for deep water renewal to occur might be shorter than the time it takes to replace all deep water, leading to a partial renewal of the basin water. There will also be some degree of mixing and entrainment during the renewal, so that some percentage of the old fjord water may remain in the basin and cause the density in the fjord after the renewal to be lower than the maximum density observed at sill level (i.e. $\rho_0 <= \rho_{coast,n}$). A partial renewal of the shallower basin water will likely affect D, while "insufficient" or partial renewal of the basin bottom water would reduce the length of the stagnation period between renewals (at least if we define a renewal to have occurred as soon as some of the bottom water has been replaced and the bottom density increased).

We applied the statistical framework to Masfjorden, a sill fjord in southwestern Norway for which D can be estimated from observations. The hydrographic data from a nearby coastal station Sognesjøen show a decreasing trend in density ($\alpha < 0$) and a (non-significant) increase in the density variability after 1990. The results suggest, that it is very likely that the length of the stagnation periods in Masfjorden during the last 30 years has increased as a consequence of the negative trend in density outside the fjord.

Aksnes et al. (2019) estimated that without deep water renewal, biological oxygen consumption will cause Masfjorden to become anoxic in 7–12 years. Our results show that the observed changes along the coast (decrease in density and potentially also increased variability) lead to a large increase (with a factor of five to ten) in the probability of stagnation periods longer than 10 years, and the likelihood for anoxic conditions at the bottom of Masfjorden then consequently increases.

Prior to the trend (before 1990) the results indicate that Masfjorden would be anoxic, i.e. the water at the bottom of the fjord would be older than 7 (12) years, 9 (0.6)% of the time. During the period with the trend (after 1990), the fjord would be anoxic 28 (8)% of the time (or 34 (12)% if the increased variability is included). While Aksnes et al. (2019) observe a decreasing trend in the oxygen concentration in Masfjorden, the fjord has so far not been observed to be completely anoxic, although values below 2 mL L^{-1} were observed in 2019 (unpublished data). The consequences of the reduced oxygen concentrations for the marine life in the fjord are discussed extensively by Aksnes et al. (2019).

The negative trend in the annual maximum density at Sognesjøen is observed at all depths (Table 1) and at five other hydrographical stations along the Atlantic coast of Norway, reaching from Lista in the south up to Skrova, east of Lofoten islands, in the north. The northernmost station Ingøy in the Barents Sea does not show any trend and neither does Eggum, located west of the Lofoten islands. While the origin of the trend is beyond the scope of this work, we note that the trend does not appear to be linked to the Atlantic Multidecadal Oscillation (Fig. 5) and that trends in the regional hydrography have been described elsewhere: Mork et al. (2019) show a warming and freshening trend in the Norwegian Sea since 2010, while Albretsen et al. (2012) showed that the mean temperature of both the surface and the deep (200 m) waters along the entire Norwegian coast had increased by more than 0.6° C between the periods 1961–1990 and 2000–2009.

The decreasing trend in the annual maximum density observed at the six hydrographic stations suggests that a reduction in the renewal rate (and as a consequence in the oxygen concentrations) must be expected, not only in Masfjorden, but also in the majority of Norwegian sill fjords. The increase in the length of the stagnation periods will depend on the strength of the trend and on the initial value of D/σ. Fjords with low values of D will be more sensitive, i.e. be more likely to experience an increase in the length of the stagnation period, than fjords with high D.

CRediT authorship contribution statement

E. Darelius: Conceptualization, Methodology, Formal analysis, Investigation, Writing - original draft, Writing - review & editing.

Declaration of competing interest

The authors declare that they have no known competing financial interests or personal relationships that could have appeared to influence the work reported in this paper.

Acknowledgments

Comments and suggestions from D. L. Aksnes, K. Daae, L. H. Smedsrud, G. Björk, K. Nordberg and three anonymous reviewers were much appreciated.

References

Aksnes, D.L., Aure, J., Johansen, P.-O., Helge, G., Salvanes, A.G.V., 2019. Multi-decadal warming of Atlantic water and associated decline of dissolved oxygen in a deep fjord. Estuar. Coast. Shelf Sci. 228, 106392. http://dx.doi.org/10.1016/j.ecss.2019.106392.

Albretsen, J., Aure, J., Sætre, R., Danielssen, D.S., 2012. Climatic variability in the Skagerrak and coastal waters of Norway. ICES J. Mar. Sci. 69 (5), 758–763. http://dx.doi.org/10.1093/icesjms/fsr187.

Arneborg, L., Erlandsson, C.P., Liljebladh, B., Stigebrandt, A., 2004. The rate of inflow and mixing during deep-water renewal in a sill fjord. Limnol. Oceanogr. 49 (3), 768–777. http://dx.doi.org/10.4319/lo.2004.49.3.0768.

Boone, W., Rysgaard, S., Carlson, D.F., Meire, L., Kirillov, S., Mortensen, J., Dmitrenko, I., Vergeynst, L., Sejr, M.K., 2018. Coastal freshening prevents fjord bottom water renewal in northeast Greenland: A mooring study from 2003 to 2015. Geophys. Res. Lett. 45 (6), 2726–2733. http://dx.doi.org/10.1002/2017GL076591.

Cottier, F.R., Nilsen, F., Skogseth, R., Tverberg, V., Skardhamar, J., Svendsen, H., 2010. Arctic fjords: a review of the oceanographic environment and dominant physical processes. Geol. Soc. Spec. Publ. 344, 35–50. http://dx.doi.org/10.1144/SP344.4.

Enfield, D.B., Mestas-Nunez, A.M., Trimble, P.J., 2001. The Atlantic Multidecadal Oscillation and its relationship to rainfall and river flows in the continental U.S.. Geophys. Res. Lett. 28.

Gade, H.G., 1973. Deep water exchanges in a sill fjord: A stochastic process. J. Phys. Oceanogr. 3 (2), 213–219. http://dx.doi.org/10.1175/1520-0485(1973)003<0213:dweias>2.0.co;2.

Gade, H., Edwards, A., 1980. Deep water renewal in fjords. In: Freeland, H., Farmer, D., Levings, C.D. (Eds.), Fjord Oceanography.

Gillibrand, P.A., Turrell, W.R., Elliot, A.J., 1995. Deep-water renewal in the Upper Basin of Loch Sunart, a Scottish fjord. J. Phys. Oceanogr. 25.

Gillibrand, P.A., Turrell, W.R., Moore, D.C., Adams, R.D., 1996. Bottom water stagnation and oxygen depletion in a Scottish sea loch. Estuar. Coast. Shelf Sci. 43 (2), 217–235. http://dx.doi.org/10.1006/ecss.1996.0066.

Gladish, C.V., Holland, D.M., Rosing-Asvid, A., Behrens, J.W., Boje, J., 2015. Oceanic boundary conditions for Jakobshavn Glacier. part i: variability and renewal of Ilulissat Icefjord waters, 2001-14. J. Phys. Oceanogr. 45 (1), 3–32. http://dx.doi.org/10.1175/JPO-D-14-0044.1.

International Council for the Exploration of the Sea, 2019. http://www.ices.dk/marine-data/data-portals/Pages/ocean.aspx (Accessed: 30-05-2019).

Mork, K.A., Skagseth, Ø., Søiland, H., 2019. Recent warming and freshening of the Norwegian Sea observed by Argo data. J. Clim. 32 (12), 3695–3705. http://dx.doi.org/10.1175/JCLI-D-18-0591.1.

NOAA Earth System Research Laboratory, 2020. https://www.esrl.noaa.gov/psd/data/timeseries/AMO/ (Accessed: 06-01-2020).

Norwegian Institute of Marine Research, 2020. www.imr.no/forskning/forskningsdata/stasjoner/view/initdownload (Accessed: 07-01-2020).

Norwegian Marine Data Center, 2019. https://nmdc.no (Accessed: 30-05-2019).

Polovodova Asteman, I., Nordberg, K., 2013. Foraminiferal fauna from a deep basin in Gullmar fjord: The influence of seasonal hypoxia and NorthAtlantic Oscillation. J. Sea Res. 79, 40–49. http://dx.doi.org/10.1016/j.seares.2013.02.001.

Rysgaard, S., Vang, T., Stjernholm, M., Rasmussen, B., Windeline, A., Kiilsholm, S., 2003. Physical conditions, carbon transport, and climate change impacts in a northeast Greenland fjord. Arct. Antarct. Alpine Res. 35 (3), 301–312.

Sejr, M.K., Stedmon, C.A., Bendtsen, J., Abermann, J., Juul-Pedersen, T., Mortensen, J., Rysgaard, S., 2017. Evidence of local and regional freshening of Northeast Greenland coastal waters. Sci. Rep. 7 (1), 7–12. http://dx.doi.org/10.1038/s41598-017-10610-9.

Stigebrandt, A., 2012. Hydrodynamics and circulation of fjords. In: Bengtsson, L., Herschy, R.W., Fairbridge, R.W. (Eds.), Encyclopedia of Lakes and Reservoirs. Springer, Dordrecht, pp. 327–344. http://dx.doi.org/10.1007/978-1-4020-4410-6_247.

Stigebrandt, A., Aure, J., 1989. Vertical mixing in basin waters of fjords. J. Phys. Oceanogr. 19.